Combustion and Flame 168 (2016) 53–64

Contents lists available at ScienceDirect

Combustion and Flame

journal homepage: www.elsevier.com/locate/combustflame

Accelerate global sensitivity analysis using artificial neural network algorithm: Case studies for combustion kinetic model

Shuang Li[a,b], Bin Yang[b,*], Fei Qi[a,c]

[a] National Synchrotron Radiation Laboratory, University of Science and Technology of China, Hefei, Anhui 230029, PR China
[b] Center for Combustion Energy and Department of Thermal Engineering, Tsinghua University, Beijing 100084, PR China
[c] Key Laboratory for Power Machinery and Engineering of M.O.E., Shanghai Jiao Tong University, Shanghai 200240, PR China

ARTICLE INFO

Article history:
Received 1 November 2015
Revised 29 March 2016
Accepted 30 March 2016
Available online 4 May 2016

Keywords:
Artificial neural network (ANN)
High dimensional model representations (HDMR)
Double-layer surrogate model
Global sensitivity analysis
Residual effect

ABSTRACT

Global sensitivity and uncertainty analyses have attracted more and more attention in recent combustion kinetic studies. However, the high computational cost hinders their application in complex kinetic models. In order to accelerate the convergence speed, the artificial neural networks (ANN) methodology is applied into two widely used quantitative sensitivity analysis methods in the present work, i.e. the Sobol' sensitivity estimation and the random sampling high dimensional model representations (RS-HDMR). An ANN is constructed and trained using original model samples, which can then be used as a surrogate model to generate numerous samples for a global sensitivity analysis with Sobol' sensitivity estimation or RS-HDMR. It is shown that the ANN greatly reduces computational costs for estimating Sobol' sensitivity indices. The performances of the proposed ANN based HDMR method (ANN-HDMR) have been tested by a widely used analytical function (Sobol' *g*-function) and two practical models in combustion (master equation kinetic model and reaction kinetic model). The results show that the ANN-HDMR only needs a few tenths of original samples in the sensitivity analysis of master equation kinetic model and premixed H_2/O_2 ignition model. The ANN-HDMR is a kind of double-layer surrogate model which couples the advantage of ANN for fast convergence and RS-HDMR for direct sensitivity indices calculation, and thus it exhibits better performance in convergence and stability comparing with the commonly used RS-HDMR.

1. Introduction

Detailed chemical kinetic modeling of pure or mixed fuels combustion enables an in-depth understanding of combustion processes and ultimately makes valuable contributions to worldwide energy production while limiting its environmental impact. Unfortunately, a complete and accurate chemical kinetic model may never exist, because it is impossible to predetermine the completeness of a kinetic model, moreover, the uncertainty of a model is too complicated so that it is very difficult to determine a unique model in the uncertainty space [1]. The development of a chemical kinetic model is thus the process of reducing the uncertainty of model prediction. According to Oberkampf and Roy [2], the sources of a kinetic model's uncertainty include model form error, numerical uncertainty and model input uncertainty. Even if we use appropriate numerical approaches to solve the mathematical equations of a structurally complete model, high uncertainty still exists in the model prediction due to the uncertainties of model input parameters including reaction rate coefficients, thermodynamic and transport parameters. Rigorous studies by experimental measurements or theoretical calculations on each input parameter will undoubtedly reduce the prediction uncertainty. However, for a complex model consisting of hundreds or even thousands of input parameters, it is impractical to accurately determine each parameter due to the prohibitively high computational or experimental costs.

A sensitivity analysis method studies how uncertainty in the output of a model can be apportioned to different sources of uncertainty in the model input [3]. It may take a local or global approach. A local sensitivity analysis explores the response of the model output to a small change of the parameter from its nominal value. Because of its high computational efficiency, the local method has been implemented in widely used chemical kinetic programs such as CHEMKIN [4], KINAL [5], Cantera [6], FlameMaster [7], laminarSMOKE [8] and OpenSMOKE++ [9]. However, if the input parameters have strong nonlinear or coupled effects on the outputs, local methods may produce misleading results. A global sensitivity analysis (GSA) estimates the effect of input parameters across the whole uncertainty space on model predictions. Many methods for GSA are used in chemical kinetic models [10,11]. Sobol' sensitivity estimation [12–14] and RS-HDMR [15–18] are two

* Corresponding author. Fax: 86-10-62796631.
E-mail address: byang@tsinghua.edu.cn (B. Yang).

http://dx.doi.org/10.1016/j.combustflame.2016.03.028
0010-2180/

common GSA methods based on analysis of variance (ANOVA) decomposition, which can quantitatively evaluate the independent and coupled effects of input parameters.

Sobol' proposed a method based on Monte Carlo sampling [12] to estimate partial variances and calculate global sensitivity indices, which is able to obtain accurate results but computational expensive. The high computational cost prohibits its application in complex chemical kinetic models, although efforts have been made in past decades to reduce the cost [19,20]. The RS-HDMR is a series of methods to construct low order ANOVA decomposition expression with assuming negligible high order interactive effects [16]. This assumption rests on the fact that one tends to choose the parameters that act the most independently for describing a physical or chemical system [16,17]. Under this assumption, the constructed RS-HDMR expression is actually an effective surrogate model of the original model. Then sensitivity indices can be easily obtained from the RS-HDMR expression. Li et al. [18] have developed several practical approaches to construct RS-HDMR expressions using a minimization process and Monte Carlo integration (named as DMC-HDMR hereafter). To reduce the computational cost and improve the accuracy in RS-HDMR expression, several optimization methods have been proposed, including the control variate methods [21,22], a method proposed by Ziehn and Tomlin which automatically chooses the best order of component functions of RS-HDMR expression [23], and a threshold method [24] used to exclude the unimportant terms. RS-HDMR combined with aforementioned three kinds of methods is named as Optimized-HDMR in this work. The Optimized-HDMR has been implemented in the program GUI_HDMR [25], and this user-friendly program has promoted the application of RS-HDMR in combustion studies. Although the Optimized-HDMR has a better convergence performance comparing with the original RS-HDMR, it may cause instability by, for example, increasing the risk of missing important terms.

As discussed above, the Sobol' sensitivity estimation and the original RS-HDMR require a lot of samples to get convergent results, which requires high computational cost for the analysis of complex combustion kinetic models. A detailed combustion kinetic model aims to describe extensive combustion properties under wide range of combustion conditions, which is the intrinsic reason for its complexity. Fortunately, sensitivity analyses are usually conducted for only a few targets under some specific conditions, thus a drastically simplified surrogate model could be feasible to represent the original combustion chemical model with adequate precision. With such a simplified surrogate model, samples can be quickly generated for a sensitivity analysis using the Sobol' sensitivity estimation or the original RS-HDMR methods. With regard to constructing surrogate models, ANN inspired by biological neural systems is a more popular method compared with RS-HDMR. Because of its powerful potential in exploring a complex model, e.g. massive parallelism, generalization capacity and fault-tolerance ability [26], ANN has been widely used in fields such as pattern recognition [27,28], reliability analysis [29,30], classification [31,32], medical diagnosis [33,34], process control [35,36] and combustion kinetic systems [37–49]. The most popular type of ANN is multilayer perceptron (MLP) feed-forward neural network. A MLP consists of three layers: input, hidden and output layer. Figure 1 illustrates a single hidden layer MLP feed-forward neural network. The back-propagation (BP) algorithm [50] is the most widely used learning algorithm for a MLP neural network. The learning process consists of two parts: feed-forward and backward pass. The outputs of the ANN are calculated in the feed-forward pass process and the output errors are propagated backward to adjust the weights and biases of the ANN.

In this study, the ANN algorithm has been combined with the Sobol' sensitivity estimation (ANN-Sobol') and the original RS-HDMR (ANN-HDMR) respectively to perform the GSA for detailed

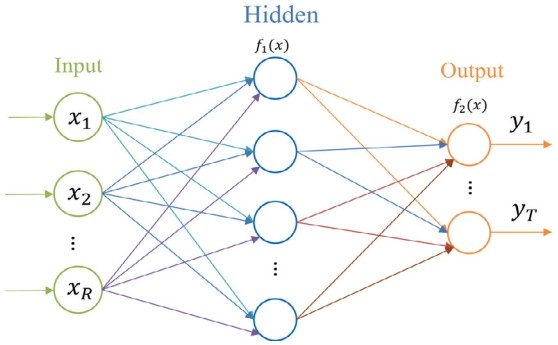

Fig. 1. Example of a single hidden layer MLP feed-forward neural network. $x_1, x_2, \ldots, x_R$ are input parameters, $y_1, \ldots, y_T$ are output targets, R is the number of input parameters, and T is the number of output targets. $f_1(x)$ is the activation function of hidden layer, and $f_2(x)$ is the activation function of output layer.

combustion kinetic models. The objective of this study is to illustrate how the ANN can reduce the computational cost remarkably of the Sobol' sensitivity estimation for kinetic models, and to provide an alternative approach to accelerate the convergence speed of RS-HDMR for GSA by coupling the advantage of ANN for fast convergence and RS-HDMR for direct sensitivity indices calculation, which is different from the Optimized-HDMR methods. Three kinds of cases including the Sobol' *g*-function, a master equation kinetic model, and a premixed H_2/O_2 ignition model were employed to compare the performances of ANN-HDMR against Optimized-HDMR. The difference between these two ANN based GSA methods was demonstrated through the sensitivity analysis of the premixed H_2/O_2 ignition model.

2. Theoretical methods

2.1. ANN based GSA (ANN-GSA) algorithm

The process of ANN-GSA is as follows: (1) Randomly generate a number of input parameters over their uncertainty ranges, and calculate the output targets using the original model. The combination of a set of input parameters and the corresponding output target is called a *sample*. (2) Train the ANN to generate a drastically simplified surrogate model from the original model using the generated samples. (3) Conduct a GSA using the well-trained ANN.

The samples generated by the original model are named as original samples, and those obtained from the well-trained ANN are named as ANN samples hereafter. Two ANN-GSA methods, ANN-Sobol' and ANN-HDMR, were developed in the present work. For ANN-Sobol', the well-trained ANN is used as a surrogate model to generate Monte Carlo samples for estimating sensitivity indices. For ANN-HDMR, the well-trained ANN is taken as the first layer surrogate model and RS-HDMR is used to construct the second layer surrogate model using the samples generated by the first layer. Figure 2 demonstrates the calculation process of ANN-HDMR: the original model is used to generate a number of original samples firstly, then two layer surrogate models are constructed to conduct the GSA.

In this work, a single hidden layer feed-forward MLP ANN was employed in ANN-HDMR and ANN-Sobol', and the back-propagation based on the Marquardt–Levenberg algorithm [51] was used as the learning algorithm. The 'tansig' [$y = 2/(1 + \exp(-2x)) - 1$] and 'purelin' ($y = x$) functions were used as the activation functions of the hidden and output layers, respectively. In the training process, 80% of the original samples were used for training, 10% were used to validate the generality of the network, and the remaining 10% were used for testing. The number of hidden layer nodes and the maximum iteration number were care-

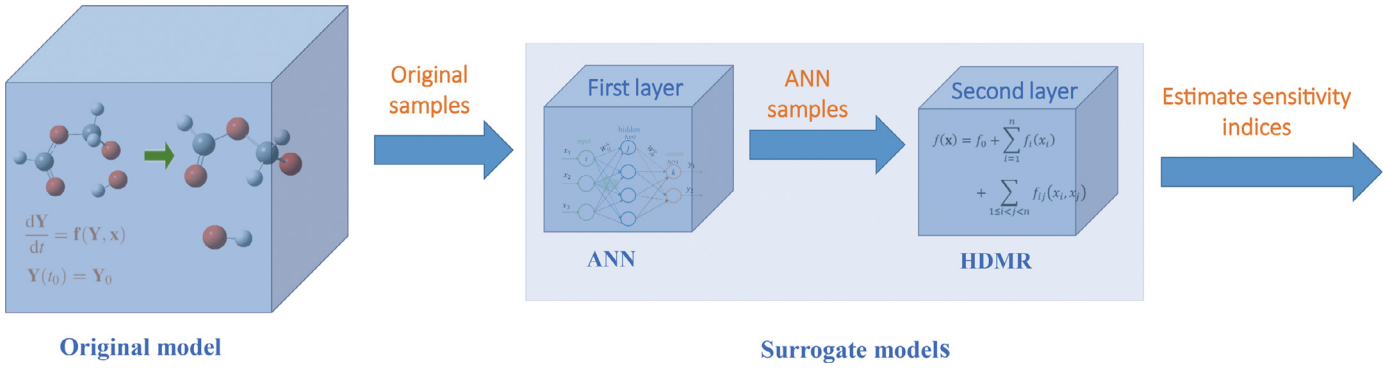

Fig. 2. Schematic diagram of the computation process of ANN-HDMR. The left cube represents the original model, the middle cube represents the first layer surrogate model which is constructed by ANN using the original samples, and the right cube represents the second layer surrogate model which is constructed by ANN RS-HDMR using the samples generated by first layer surrogate model.

fully chosen to overcome the over-fitting and under-fitting problems. Over-fitting means that a trained ANN has weak capability of generalization. An over-fitted ANN usually has a good prediction capability over training samples, but has a bad prediction capability over testing samples. Under-fitting means that a trained ANN is too simple to be capable of representing the relationship between input parameters and output targets. An under-fitted ANN usually has bad prediction capabilities over both training and testing samples. The methods to improve the generalization capability of the ANN can be found in references [52, 53]. To facilitate further discussion, some theoretical description of the Sobol' sensitivity estimation used in ANN-Sobol' and the RS-HDMR used in ANN-HDMR are provided as follows.

Both Sobol' sensitivity estimation and RS-HDMR are based on the idea of ANOVA decomposition. If $f(\mathbf{x})$ is a square-integrable function defined in the unit hypercube $K^n = [0,1]^n$, it is possible to represent $f(\mathbf{x})$ in a form [54]:

$$f(\mathbf{x}) = f_0 + \sum_{i=1}^{n} f_i(x_i) + \sum_{1\le i<j\le n} f_{ij}(x_i, x_j) + \cdots + f_{1,2\ldots n}(x_1, x_2, \ldots, x_n) \tag{1}$$

where n is the number of input parameters, f_0 is the zeroth order component function which represents the mean effect to $f(\mathbf{x})$, $f_i(x_i)$ is the first order component function which represents independent effects of input parameter x_i to $f(\mathbf{x})$, $f_{ij}(x_i, x_j)$ is the second order component function which represents correlated effects to $f(\mathbf{x})$ by both x_i and x_j. $f_{1,2\ldots n}(x_1, x_2, \ldots, x_n)$ represents the nth correlated effects to $f(\mathbf{x})$. If the following property is imposed on Eq. (1), then Eq. (1) becomes the ANOVA-representation [55] of $f(\mathbf{x})$.

$$\int_0^1 f_{i_1\ldots i_s}\left(x_{i_1,\ \ldots,i_s}\right)dx_k = 0, \quad \text{for } k = i_1, \ldots, i_s, \ 1 \le i_1 < \ldots < i_s \le n \tag{2}$$

Sobol' [12,14] has provided a Monte Carlo based method to estimate partial variances. The mean value of $f(\mathbf{x})$ is estimated as:

$$f_0 \approx \frac{1}{N}\sum_{m=1}^{N} f(\boldsymbol{x}_m) \tag{3}$$

where N is the sample size of the Monte Carlo simulations. The total variance D and the first order partial variance D_i can be estimated as:

$$D \approx \frac{1}{N}\sum_{m=1}^{N} f^2(\boldsymbol{x}_m) - {f_0}^2 \tag{4}$$

$$D_i \approx \frac{1}{N}\sum_{m=1}^{N} f\left(\boldsymbol{u}_m^{-i}, x_{im}\right) f\left(\boldsymbol{v}_m^{-i}, x_{im}\right) - {f_0}^2 \tag{5}$$

Here $\boldsymbol{u}_m^{-i}$ and $\boldsymbol{v}_m^{-i}$ refer to different Monte Carlo samples generated on K^{n-1}(K^n minus the input parameter x_i). Furthermore, the second order partial variance D_{ij} can be estimated by combining total variance and first order variance:

$$D_{ij} \approx \frac{1}{N}\sum_{m=1}^{N} f\left(\boldsymbol{u}_m^{-ij}, x_{im}, x_{jm}\right) f\left(\boldsymbol{v}_m^{-ij}, x_{im}, x_{jm}\right) - D_i - D_j - {f_0}^2 \tag{6}$$

By analogy, we can estimate each partial variance. Another useful measurement is the total effect (or total sensitivity) introduced by Homma and Saltelli [13]. The total variance D_{Ti} of parameter x_i is the sum of partial variances including x_i.

$$D_{Ti} = D - \left(\frac{1}{N}\sum_{m=1}^{N} f(x_{im}, \boldsymbol{u}_m) f\left(x'_{im}, \boldsymbol{u}_m\right) - f_0^2\right) \tag{7}$$

The variances of individual input parameters and parameter interactions to the total output variance are defined as variance-based global sensitivity indices as:

$$S_{i_1\ldots i_s} = \frac{D_{i_1\ldots i_s}}{D} \tag{8}$$

Alis and Rabitz [17] presented an algorithm to construct a low order ANOVA decomposition expression with a set of randomly sampled data, termed RS-HDMR. Li et al. [18] introduced several practical approaches to construct RS-HDMR component functions. Among three different analytical basis functions used to approximate the component functions, the orthonormal polynomials provided the best accuracy.

We use the method developed by Li et al. [18] to construct RS-HDMR expression with the orthonormal polynomials as:

$$\varphi_1(x) = \sqrt{3}(2x-1) \tag{9}$$

$$\varphi_2(x) = 6\sqrt{5}\left(x^2 - x + \frac{1}{6}\right) \tag{10}$$

$$\varphi_3(x) = 20\sqrt{7}\left(x^3 - \frac{3}{2}x^2 + \frac{3}{5}x - \frac{1}{20}\right) \tag{11}$$

...

which satisfy

$$\int_0^1 \varphi_k(x)\ dx = 0, \quad k = 1,\ 2,\ \ldots \tag{12}$$

$$\int_0^1 \varphi_k{}^2(x)\ dx = 1,\ \ k = 1,\ 2,\ \ldots \tag{13}$$

$$\int_0^1 \varphi_k(x)\varphi_l(x)\ dx = 0,\ \ k \neq l \tag{14}$$

For most systems, the HDMR expression up to the second-order can provide a satisfactory approximation for $f(\mathbf{x})$ [56], then the ANOVA decomposition expression can be expressed as:

$$f(\mathbf{x}) = f_0 + \sum_{i=1}^{n}\sum_{r=1}^{k}\alpha_r^i\varphi_r(x_i) + \sum_{1\le i<j\le n}\sum_{p=1}^{k1}\sum_{q=1}^{k2}\beta_{pq}^{ij}\varphi_p(x_i)\varphi_q\left(x_j\right) \tag{15}$$

The coefficients α_r^i and β_{pq}^{ij} [17,18] are determined by a minimization process and Monte Carlo integration:

$$\alpha_r^i \approx \frac{1}{N}\sum_{s=1}^{N} f(\boldsymbol{x}^s)\varphi_r\left(x_i^s\right) \tag{16}$$

$$\beta_{pq}^{ij} \approx \frac{1}{N}\sum_{s=1}^{N} f(\boldsymbol{x}^s)\varphi_p\left(x_i^s\right)\varphi_q\left(x_j^s\right) \tag{17}$$

The partial variances can be calculated by:

$$D_i = \sum_{r=1}^{k}\left(\alpha_r^i\right)^2 \tag{18}$$

$$D_{ij} = \sum_{p=1}^{k1}\sum_{q=1}^{k2}\left(\beta_{pq}^{ij}\right)^2 \tag{19}$$

The sensitivity indices can be consequently estimated by Eq. (8).

The generalizability of the surrogate model constructed by ANN-HDMR is affected by the representativeness of the original sample set, the generalizability of the first layer surrogate model (ANN) and the second layer surrogate model (HDMR). The representativeness means that the original sample set is a fairly accurate reflection of the parameter uncertainty space from which the samples are drawn. The representativeness of the original sample set is related to the sampling method and the sample size. Quasi-random low-discrepancy sequences can obtain more representative sample sets than random sequences. In this work, the input parameters were assumed to follow uniform distribution within uncertainty range in all cases, therefore Sobol' quasi-random sequence was used to obtain representative sample set. To examine the generalizability of the first and second layer surrogate models, the original sample set was divided into the training set, the validation set and the test set. If both the first and second layer surrogate models have good prediction abilities over the three sets of samples, and the original sample size is large enough to make sure the sensitivity results are independent of it, the surrogate model constructed by the ANN-HDMR method is regarded to be generalizable.

2.2. Residual effect

The number of the component functions of the ANOVA-representation of $f(\mathbf{x})$ in Eq. (1) grows exponentially with the number of input parameters, while most of the component functions have negligible effects on $f(\mathbf{x})$. To select important terms and reduce the computational costs for calculating sensitivity indices, residual effect is proposed in this work. Residual effect of the parameter x_i is defined as the total effect of x_i minus all sensitivity indices involving the x_i which have been calculated. Residual effect is calculated as follows:

$$\mathrm{RS}_i^1 = S_{Ti} \tag{20}$$

$$\mathrm{RS}_i^2 = S_{Ti} - S_i \tag{21}$$

$$\mathrm{RS}_i^3 = S_{Ti} - S_i - \mathrm{S}_{ci} \tag{22}$$

Here RS_i^1, RS_i^2, RS_i^3 are residual effects of parameter x_i in the first, second and third step, respectively. S_{Ti} represents the total effect of parameter x_i, S_i is the first order sensitivity index of x_i, and S_{ci} represents the sum of all the second order sensitivity indices, which involve the parameter x_i. In the first step, residual effect of parameter x_i is equal to the total effect of x_i. A threshold T_1 is selected and the first order terms whose residual effects greater than T_1 will be calculated. RS_i^2 is the residual effect of parameter x_i in the second step, which is determined by subtracting the first order sensitivity of x_i from the total effect of x_i. If both RS_i^2 and RS_j^2 are larger than a threshold T_2, then the second order sensitivity $S_{i,j}$ will be computed. By analogy, the third order sensitivity $S_{i,j,k}$ will be calculated if $\mathrm{RS}_i^3 \ge T_3$, $\mathrm{RS}_j^3 \ge T_3$ and $\mathrm{RS}_k^3 \ge T_3$, where T_3 is threshold for the third order.

2.3. Software overview

A fully functional program ANN_GSA_Tool for global sensitivity and uncertainty analysis based on ANN-HDMR and ANN- Sobol' was developed, which includes a MATLAB graphical user interface. The Neural Network Toolbox of MATLAB was used to implement the ANN algorithm. ANN_GSA_Tool provides the ability to calculate sensitivity indices up to the third order and the total effects, plot component functions, estimate the variance of model output, and so on. Important sensitivity indices and the distribution of model output can be displayed on the main interface. A screenshot of the main interface of ANN_GSA_Tool is provided in *Supplemental Materials*. The program and the user document are available by request. The ANN_GSA_Tool also can implement DMC-HDMR calculations. The Optimized-HDMR calculations were performed using GUI-HDMR [25], a widely used program for global sensitivity analysis.

3. Test cases

Three test cases were used to illustrate the performance of ANN-GSA, especially in the field of combustion kinetic study. The first case is the classical analytical function—Sobol' *g*-function, the second is the master equation kinetic model for pressure-dependent rate constants calculation, and the last one is the reaction kinetic model of H_2/O_2 ignition.

3.1. Sobol' g-function

Sobol' *g*-function was introduced by Saltelli and Sobol' [57], which was defined as:

$$f(\mathbf{x}) = \prod_{i=1}^{n} g_i(x_i) \tag{23}$$

where

$$g_i(x_i) = \frac{|4x_i - 2| + a_i}{1 + a_i},\ \ a_i \ge 0,$$

where a_i is an always positive constant and x_i is uniformly distributed in [0, 1]. All the first and higher order sensitivity indices can be calculated analytically. The importance of input parameter x_i is determined by the value of a_i. The larger the value of a_i, the less important of x_i. Due to the complexity and analyzability of this function, it has been widely used to measure performances of various GSA methods [25,58–62].

3.2. Master equation kinetic model

The Rice–Ramsberger–Kassel–Marcus (RRKM)/master equation (ME) method is the most popular modeling framework to predict phenomenological pressure-dependent rate coefficients for unimolecular reaction networks [63–70]. The accuracy of RRKM/ME

Table 1
The nominal values and uncertainties of input parameters used in the sensitivity analysis on the simplified reaction system of ethanol decomposition, taken from reference [72].

Index	Parameters	Value
1	C_2H_5OH energy (kcal/mol)	0 ± 1.0
2	CH_3 + CH_2OH energy (kcal/mol)	85.6 ± 1.0
3	C_2H_4 + H_2O energy (kcal/mol)	9.7 ± 1.0
4	TS2 energy (kcal/mol)	77.3 ± 2.0
5	TS1 energy (kcal/mol)	66.0 ± 2.0
6	C_2H_5OH $\langle\Delta E\rangle_{down}$ prefactor (cm^{-1})	125 ± 62.5 (±50%)
7	C_2H_5OH $\langle\Delta E\rangle_{down}$ T-exponent	0.85 ± 0.15
8	C_2H_5OH L-J: σ (Å)	4.3 ± 0.86 (±20%)
9	Ar L-J: σ (Å)	3.5 ± 0.7 (±20%)
10	C_2H_5OH L-J: $\mathcal{E}$ (K)	450.2 ± 90 (±20%)
11	Ar L-J: ε (K)	113.5 ± 22.7 (±20%)
12	C_2H_5OH hindered rotor barrier height (kcal/mol)	1.5 ± 0.15 (±10%)
13	C_2H_5OH RRHO frequency 1 (cm^{-1})	272.9 ± 27.3 (±10%)
14	C_2H_5OH RRHO frequency 2 (cm^{-1})	416.5 ± 41.7 (±10%)
15	TS2 RRHO frequency 1 (cm^{-1})	142.7 ± 14.3 (±10%)
16	TS2 RRHO frequency 2 (cm^{-1})	255.5 ± 25.6 (±10%)
17	TS2 RRHO frequency 3 (cm^{-1})	342.6 ± 34.3 (±10%)
18	TS2 RRHO frequency 4 (cm^{-1})	356.0 ± 35.6 (±10%)
19	TS2 hindered rotor barrier height (kcal/mol)	1.56 ± 0.16 (±10%)
20	TS2 imaginary frequency (cm^{-1})	246.8 ± 49.4 (±20%)
21	TS1 RRHO frequency 1 (cm^{-1})	242.3 ± 24.2 (±10%)
22	TS1 imaginary frequency (cm^{-1})	1966.5 ± 393 (±20%)

rate coefficients is strongly affected by the uncertainty of input parameters such as energy barriers, vibrational frequencies, collisional energy transfer parameters, etc. The uncertainty propagation from the input parameters to the RRKM/ME rate coefficients has been analyzed by the RS-HDMR method [71,72]. In our previous work [72], we conducted GSA using Optimized-HDMR on a simplified reaction system of ethanol decomposition. For each pair of temperature and pressure, a successful convergence required at least 20,000 samples. The Optimized-HDMR simulations took over 10 days using about 100 CPU cores. Reducing the required sample size is desired for extending our ability to explore more complicated reaction systems under various pressures and temperatures.

Two dominant reaction channels of ethanol decomposition were considered in our previous study [72]:

$$CH_3CH_2OH \rightarrow C_2H_4 + H_2O \quad (R1)$$

$$CH_3CH_2OH \rightarrow CH_3 + CH_2OH \quad (R2)$$

The C–C bond dissociation channels were studied with the canonical variational transition state theory (CVT). For each temperature, the variational transition state was specified as the geometry giving the minimum in the high pressure limit (HPL) rate constant. The master equation using the RRKM theory calculated microcanonical rate constants for these variational transition states, as well as for the tight transition state of the H_2O elimination channel. All the kinetic calculations were performed using the MESMER program [73]. More detailed information about the kinetic calculations can be found in reference [72].

Twenty-two input parameters including reactant and transition state energies, vibration frequencies, and energy transfer parameters were considered in the GSA. Nominal values and uncertainties of the twenty two input parameters are listed in Table 1. Input parameters are uniformly distributed in their uncertainty ranges. In order to compare the performance of the commonly used Optimized-HDMR method and ANN-HDMR, we conducted a GSA under 1700 K and 1 atm for this reaction system. The natural logarithm of rate constant ($\ln k$) was selected as the target for GSA by both methods. In our previous study [72], we found that the convergence speed of GSA using Optimized-HDMR was slow under this condition. Therefore, this condition was selected on purpose to test the capability of ANN-HDMR. To construct a surrogate model of master equation kinetic model using the ANN, the reactant and transition state energies etc. were used as the input parameters, and the $\ln k$ was used as the output target of the ANN. The structure of an ANN algorithm can be seen in Fig. 1. The error of $\ln k$ between the simulation result of ME kinetic model and the output of ANN is propagated backward, providing clues to weights and biases adjustment. Consequently, we are able to get a well-trained ANN representing the master equation kinetic model under 1700 K and 1 atm.

3.3. Premixed H_2/O_2 ignition model

The ignition delay time of H_2/O_2 system at $T = 1000$ K, $P = 1.59$ bar was chosen as a test target for the following reasons:

(1) Ignition delay time is an important combustion property.
(2) H_2/O_2 system is relatively small, which makes it easy to generate numerous original samples to obtain convergent results using DMC-HDMR.
(3) This model has high second order effects under such condition according to a previous study [74], which helps to distinguish the performances of different GSA methods.

Konnov [75] has updated a hydrogen combustion mechanism (including 10 species and 33 reversible reactions), with evaluating the uncertainty of each rate coefficients. This mechanism was employed in this work. The uncertainty factor (UF) of the rate coefficient was defined as:

$$\mathrm{UF} = \frac{k_0}{k_{\min}} = \frac{k_{\max}}{k_0} \quad (24)$$

where k_0 was the nominal value, $k_{\max}$ and $k_{\min}$ were the upper and lower bounds of the rate coefficient, respectively. Only the uncertainty of the A-factors of rate coefficients was taken into account. The uncertainty factors for the 33 reversible reactions (including duplicate reactions) were listed in Table 2. Each rate coefficient k_i was assumed to follow a log-uniform distribution, i.e. $\log(k_i)$ was uniformly distributed within $[\log(k_{\min}), \log(k_{\max})]$. The input parameter sets were generated using the Sobol' quasi-random sequence [76]. All the numerical simulations were carried out under constant volume adiabatic conditions using Cantera [6]. The simulated ignition delay time was defined as the time between the starting time and the moment of maximum change rate of OH concentration ($\max(\frac{d_{OH}}{d_t})$).

4. Results and discussion

In this section, the performances of ANN-HDMR and Optimized-HDMR were compared using the aforementioned three cases, while the performances of ANN-Sobol' and Sobol' sensitivity estimation were compared only for the H_2/O_2 ignition model. Besides, the comparisons between two proposed ANN based GSA methods, ANN-HDMR and ANN-Sobol', were also illustrated.

For practical models in the combustion field, the computational cost for getting original samples is much higher than that for getting ANN samples. Therefore, the required original sample size is taken as the criteria in evaluating the performances of different methods. For each case, appropriate settings of parameters were chosen for different algorithms. For Optimized-HDMR, the settings in the case of Sobol' g-function were chosen according to reference [25]. For the cases of the master equation kinetic model and the premixed H_2/O_2 ignition model, a number of parameter settings were tested, and the appropriate settings for Optimized-HDMR were chosen according to the accuracy of RS-HDMR expansion and the sum of sensitivity indices.

Table 2
The uncertainty factors for 33 reversible reactions (including duplicate reactions) of H_2/O_2 kinetic mechanism [75].

Index	Reaction	UF
1	$H+H+M \Leftrightarrow H_2+M$	2.0
2	$H+H+H_2 \Leftrightarrow H_2+H_2$	2.5
3	$H+H+N_2 \Leftrightarrow H_2+N_2$	3.2
4	$H+H+H \Leftrightarrow H_2+H$	3.2
5	$O+O+M \Leftrightarrow O_2+M$	2.0
6	$O+H+M \Leftrightarrow OH+M$	3.0
7	$H_2O+M \Leftrightarrow H+OH+M$	2.0
8	$H_2O+H_2O \Leftrightarrow H+OH+H_2O$	2.0
9	$H+O_2 (+M) \Leftrightarrow HO_2 (+M)$	1.2
10	$H+O_2 (+AR) \Leftrightarrow HO_2 (+AR)$	1.2
11	$H+O_2 (+O_2) \Leftrightarrow HO_2 (+O_2)$	1.2
12	$H+O_2 (+H_2O) \Leftrightarrow HO_2 (+H_2O)$	1.4
13	$OH+OH (+M) \Leftrightarrow H_2O_2 (+M)$	2.5
14	$OH+OH (+H_2O) \Leftrightarrow H_2O_2 (+H_2O)$	2.5
15	$O+H_2 \Leftrightarrow OH+H$	1.3
16	$H+O_2 \Leftrightarrow OH+O$	1.5
17	$H_2+OH \Leftrightarrow H_2O+H$	2.0
18	$OH+OH \Leftrightarrow H_2O+O$	1.5
19	$HO_2+O \Leftrightarrow OH+O_2$	1.2
20	$H+HO_2 \Leftrightarrow OH+OH$	2.0
21	$H+HO_2 \Leftrightarrow H_2O+O$	3.0
22	$H+HO_2 \Leftrightarrow H_2+O_2$	2.0
23	$H_2+O_2 \Leftrightarrow OH+OH$	3.0
24	$HO_2+OH \Leftrightarrow H_2O+O_2$ (duplicate)	3.0
25	$HO_2+OH \Leftrightarrow H_2O+O_2$ (duplicate)	3.0
26	$HO_2+HO_2 \Leftrightarrow H_2O_2+O_2$ (duplicate)	2.5
27	$HO_2+HO_2 \Leftrightarrow H_2O_2+O_2$ (duplicate)	1.4
28	$HO_2+HO_2+M \Leftrightarrow H_2O_2+O_2+M$	1.4
29	$H_2O_2+H \Leftrightarrow HO_2+H_2$	3.0
30	$H_2O_2+H \Leftrightarrow H_2O+OH$	2.0
31	$H_2O_2+O \Leftrightarrow HO_2+OH$	3.0
32	$H_2O_2+OH \Leftrightarrow HO_2+H_2O$ (duplicate)	2.0
33	$H_2O_2+OH \Leftrightarrow HO_2+H_2O$ (duplicate)	2.0

The estimation of the convergence of GSA depends on how accurate the sensitivity results are needed. In this work, the results of GSA are considered to have converged if the variation of the sum of sensitivity indices with the sample size is less than 0.05, and the variation of each sensitivity index of important parameter is less than 0.005. For the case where the true values of sensitivity indices can be obtained, the sum of absolute errors of important first and second order sensitivity indices is a direct criterion to indicate convergence precision of global sensitivity analysis, defined as:

$$\text{Error} = \sum_i \left|S_i - S_i^t\right| + \sum_{i,j} \left|S_{i,j} - S_{i,j}^t\right| \tag{25}$$

Here S_i is the calculated first order sensitivity index and S_i^t represents its true value. $S_{i,j}$ and $S_{i,j}^t$ are calculated and true values of the second order sensitivity indices of x_i and x_j, respectively. Using the "Error" criteria, we can compare the required original sample sizes of different GSA methods when the results of GSA reach specific precisions. All the computation is performed on the computer which consists of two Intel E5-2687w processors and 64 GB of memory.

4.1. Sobol' g-function

For the Sobol' g-function, the greater the value of a_i, the smaller the variance from the input parameter x_i, and the more difficult to accurately estimate the sensitivity index. Two different scenarios using $a_i = \{4.5, 4.5, 1, 0, 1, 9, 0, 9\}$ and $a_i = \{5000, 5500, 6000, 6500, 7000, 7500, 8000, 8500\}$ were chosen. The first scenario was frequently used in previous studies [25,62]. Each a_i in the second scenario is larger than that in the first one, putting forward higher requirements for GSA methods. For the Optimized-HDMR, the maximum polynomial orders for the first and second order component functions were set to be 10 and 5, respectively. The correlation method for variance reduction was applied, while the number of iterations was set to be 20 for both the first and second component functions. No thresholds were applied to Optimized-HDMR and ANN-HDMR. The Sobol' quasi-random sequence was taken as the sampling method for getting original samples and ANN samples. For g-function, the true values of all the first and second order sensitivity indices can be calculated analytically.

4.1.1. The first scenario

In this scenario, it is shown that 131,072 ANN samples of ANN-HDMR are enough to get stable results. More detailed information about the parameter settings of ANN-HDMR including the number of hidden layer nodes and the maximum number of iteration, is provided in *Supplemental Materials*. Table 3 lists the eight first order and top five second order sensitivity indices varying with original sample sizes using DMC-HDMR. Analytical values for the first and second order sensitivity indices are also listed. Table 4 shows the sensitivity indices using Optimized-HDMR and ANN-HDMR. The sensitivity indices of all the first order and top five second order terms were considered as important sensitivity indices. By comparing Table 3 with Table 4, one can see that both Optimized-HDMR and ANN-HDMR converge faster than DMC-HDMR. To reduce the Error to below 5%, DMC-HDMR needs 8192 samples, while Optimized-HDMR and ANN-HDMR need 4096 and 2048 original samples, respectively. From another perspective, the accuracy of the results obtained from 8192 samples using ANN-HDMR is better than that using Optimized-HDMR with the same level of CPU time. This case indicates that the ANN algorithm can accelerate the convergence of RS-HDMR similarly as the commonly used optimization methods of RS-HDMR. The DMC-HDMR needs only 8192 samples to reduce the Error to below 5%, indicating unobvious effects of accelerating convergence by the optimization methods in this case.

4.1.2. The second scenario

In this scenario, 1,048,576 ANN samples are enough for ANN-HDMR to get stable results. Because the second and higher order terms have negligible effects on the output variance, only the top eight first order sensitivity indices were taken as the important sensitivity indices. Table 5 shows that DMC-HDMR needs 524,288 samples to reduce the Error to below 5%, which is much larger than the 8192 samples in the first scenario. For this scenario, optimization algorithm is greatly needed to accelerate convergence speed because the DMC-HDMR converges very slowly. Results for sensitivity analysis using Optimized-HDMR and ANN-HDMR with various original sample sizes are listed in Table 6. It illustrates that 131,072 original samples are required to reduce the Error to below 5% for Optimized-HDMR while only 512 samples are needed for ANN-HDMR. The required sample size of ANN-HDMR is just 1/256 of the Optimized-HDMR and 1/1024 of the DMC-HDMR. In this case, both Optimized-HDMR and ANN-HDMR have faster convergence speed than DMC-HDMR, and ANN-HDMR has a better performance than Optimized-HDMR.

4.2. Master equation kinetic model

In this case, for both Optimized-HDMR and ANN-HDMR, the maximum polynomial order for the first and the second order component functions were set to be 5 and 3, respectively. The correlation method was applied to Optimized-HDMR and the number of iterations was set to be 10 for both the first and second component functions. For ANN-HDMR, ANN sample size was set to be 131,072, which has been checked to be good for getting stable results.

Table 3
Sensitivity indices of important first and second order for the Sobol' g-function with $a_i = \{4.5, 4.5, 1, 0, 1, 9, 0, 9\}$ using DMC-HDMR. S_i represents the first order sensitivity index of parameter x_i; $S_{i,j}$ represents the second order sensitivity index of parameter x_i and x_j; Sum(S_i) is the sum of all first order sensitivity indices; Sum($S_{i,j}$) is the sum of all second order sensitivity indices; Sum($S_i + S_{i,j}$) is the sum of all first and second order sensitivity indices. Error is calculated according to Eq. (25).

N	DMC-HDMR								Analytical
	1024	2048	4096	8192	16,384	32,768	65,536	131,072	
S_1	0.0289	0.0158	0.0127	0.0104	0.0103	0.0097	0.0097	0.0096	0.0096
S_2	0.0191	0.0120	0.0099	0.0098	0.0097	0.0097	0.0096	0.0096	0.0096
S_3	0.0809	0.0759	0.0746	0.0725	0.0726	0.0725	0.0725	0.0725	0.0727
S_4	0.2824	0.2792	0.2811	0.2866	0.2875	0.2896	0.2899	0.2901	0.2906
S_5	0.0827	0.0732	0.0729	0.0718	0.0720	0.0724	0.0725	0.0725	0.0727
S_6	0.0150	0.0058	0.0037	0.0030	0.0029	0.0029	0.0029	0.0029	0.0029
S_7	0.2849	0.2783	0.2797	0.2867	0.2879	0.2896	0.2899	0.2901	0.2906
S_8	0.0317	0.0147	0.0121	0.0038	0.0034	0.0029	0.0029	0.0029	0.0029
Sum(S_i)	0.8256	0.7548	0.7467	0.7446	0.7463	0.7494	0.7500	0.7502	0.7516
$S_{4,7}$	0.2346	0.1396	0.1042	0.0950	0.0935	0.0937	0.0938	0.0939	0.0969
$S_{3,4}$	0.2007	0.0809	0.0349	0.0253	0.0245	0.0235	0.0235	0.0235	0.0242
$S_{3,7}$	0.2195	0.0591	0.0351	0.0256	0.0245	0.0235	0.0235	0.0235	0.0242
$S_{4,5}$	0.1757	0.0709	0.0417	0.0285	0.0260	0.0237	0.0236	0.0235	0.0242
$S_{5,7}$	0.1892	0.0584	0.0337	0.0247	0.0238	0.0236	0.0235	0.0235	0.0242
Sum($S_{i,j}$)	6.0322	1.8875	0.5976	0.3083	0.2394	0.2180	0.2156	0.2145	0.2209
Sum($S_i + S_{i,j}$)	6.8578	2.6422	1.3443	1.0529	0.9857	0.9674	0.9656	0.9647	0.9725
Error	0.9278	0.2658	0.0919	0.0202	0.0140	0.0083	0.0077	0.0073	0.0000

Table 4
Sensitivity indices of important first and second order for the Sobol' g-function with $a_i = \{4.5, 4.5, 1, 0, 1, 9, 0, 9\}$ using Optimized-HDMR and ANN-HDMR.

N	Optimized-HDMR				ANN-HDMR				Analytical
	1024	2048	4096	8192	1024	2048	4096	8192	
S_1	0.0126	0.0142	0.0122	0.0103	0.0080	0.0094	0.0092	0.0095	0.0096
S_2	0.0100	0.0095	0.0095	0.0097	0.0095	0.0097	0.0094	0.0096	0.0096
S_3	0.0680	0.0706	0.0729	0.0724	0.0658	0.0741	0.0712	0.0724	0.0727
S_4	0.2732	0.2741	0.2784	0.2865	0.2825	0.2878	0.2903	0.2897	0.2906
S_5	0.0725	0.0710	0.0723	0.0718	0.0698	0.0702	0.0714	0.0725	0.0727
S_6	0.0000	0.0000	0.0000	0.0027	0.0011	0.0026	0.0028	0.0029	0.0029
S_7	0.2675	0.2766	0.2792	0.2866	0.2898	0.2903	0.2920	0.2898	0.2906
S_8	0.0068	0.0051	0.0044	0.0036	0.0023	0.0025	0.0027	0.0028	0.0029
Sum(S_i)	0.7105	0.7211	0.7289	0.7437	0.7288	0.7466	0.7491	0.7491	0.7516
$S_{4,7}$	0.0763	0.0888	0.0919	0.0926	0.0985	0.0935	0.0949	0.0942	0.0969
$S_{3,4}$	0.0222	0.0227	0.0245	0.0238	0.0222	0.0241	0.0231	0.0235	0.0242
$S_{3,7}$	0.0208	0.0232	0.0251	0.0238	0.0231	0.0243	0.0233	0.0234	0.0242
$S_{4,5}$	0.0175	0.0203	0.0246	0.0233	0.0241	0.0226	0.0232	0.0236	0.0242
$S_{5,7}$	0.0199	0.0214	0.0244	0.0233	0.0248	0.0229	0.0234	0.0235	0.0242
Sum($S_{i,j}$)	0.1688	0.1931	0.2138	0.2161	0.2224	0.2146	0.2140	0.2149	0.2209
Sum($S_i + S_{i,j}$)	0.8793	0.9142	0.9427	0.9598	0.9512	0.9612	0.9631	0.9640	0.9725
Error	0.0925	0.0613	0.0381	0.0180	0.0510	0.0196	0.0137	0.0106	0.0000

Table 5
Sensitivity indices of important first and second order for the Sobol' g-function with $a_i = \{5000, 5500, 6000, 6500, 7000, 7500, 8000, 8500\}$ using DMC-HDMR. Sensitivity indices of all first order terms are chosen as important sensitivity indices.

N	DMC-HDMR								Analytical
	4096	8192	16,384	32,768	65,536	131,072	262,144	524,288	1,048,576	
S_1	51.41	13.01	3.410	1.009	0.4083	0.2578	0.2203	0.2109	0.2086	0.2081
S_2	51.41	12.97	3.372	0.9720	0.3718	0.2218	0.1842	0.1749	0.1725	0.1720
S_3	51.39	12.94	3.345	0.9446	0.3444	0.1943	0.1568	0.1474	0.1451	0.1446
S_4	51.32	12.92	3.324	0.9232	0.3230	0.1730	0.1355	0.1261	0.1238	0.1232
S_5	51.32	12.91	3.306	0.9062	0.3061	0.1560	0.1185	0.1092	0.1068	0.1062
S_6	51.38	12.89	3.292	0.8926	0.2924	0.1424	0.1049	0.0955	0.0931	0.0925
S_7	51.31	12.88	3.283	0.8814	0.2812	0.1312	0.0937	0.0843	0.0820	0.0813
S_8	51.30	12.89	3.279	0.8721	0.2720	0.1219	0.0844	0.0750	0.0727	0.0720
Sum(S_i)	410.8	103.4	26.61	7.4010	2.5990	1.3980	1.0980	1.0230	1.0050	1.0000
Error	409.8	102.4	25.61	6.4010	1.5990	0.3984	0.0983	0.0233	0.0046	0.0000

Sensitivity analysis results show that the first order terms dominate the uncertainty of rate constants under this condition (the sum of first order sensitivity indices can reach about 0.99 for reactions R1 and R2). Figure 3 shows the first order sensitivity indices of the top four important parameters and the sum of the first order sensitivity indices of reaction rates of R1 and R2 versus the original sample sizes using Optimized-HDMR and ANN-HDMR. It illustrates that only 100 original samples are enough for ANN-HDMR to identify the first four most important parameters of R1 and R2 and produce the correct ranking. The efficiency of ANN-HDMR is even comparable with semi-quantitative methods of GSA such as the Morris method in this case. The optimized-HDMR method needs about 10,000 samples to obtain stable and precise results while ANN-HDMR just needs about 200 original samples. It

Table 6
Sensitivity indices of important first and second order for the Sobol' g-function a_i={5000, 5500, 6000, 6500, 7000, 7500, 8000, 8500} using Optimized-HDMR and ANN-HDMR.

N	Optimized-HDMR						ANN-HDMR			Analytical
	16,384	32,768	65,536	131,072	262,144	524,288	256	512	1024	
S_1	0.1953	0.1951	0.1951	0.2049	0.2049	0.2069	0.1530	0.2099	0.2096	0.2081
S_2	0.0000	0.1613	0.1613	0.1693	0.1693	0.1710	0.1406	0.1746	0.1718	0.1720
S_3	0.0000	0.1355	0.1355	0.1423	0.1423	0.1437	0.0855	0.1422	0.1436	0.1446
S_4	0.0000	0.1155	0.1155	0.1155	0.1213	0.1224	0.0874	0.1235	0.1259	0.1232
S_5	0.0000	0.0996	0.0996	0.0996	0.1046	0.1056	0.0699	0.1038	0.1058	0.1062
S_6	0.0000	0.0867	0.0867	0.0867	0.0911	0.0920	0.0934	0.0941	0.0926	0.0925
S_7	0.0000	0.0762	0.0762	0.0762	0.0800	0.0808	0.0640	0.0802	0.0813	0.0813
S_8	0.0000	0.0675	0.0675	0.0675	0.0709	0.0716	0.0636	0.0705	0.0735	0.0720
Sum(S_i)	0.1953	0.9375	0.9375	0.9621	0.9844	0.9939	0.7574	0.9989	1.0041	1.0000
Error	0.8047	0.0625	0.0625	0.0379	0.0156	0.0061	0.2445	0.0136	0.0073	0.0000

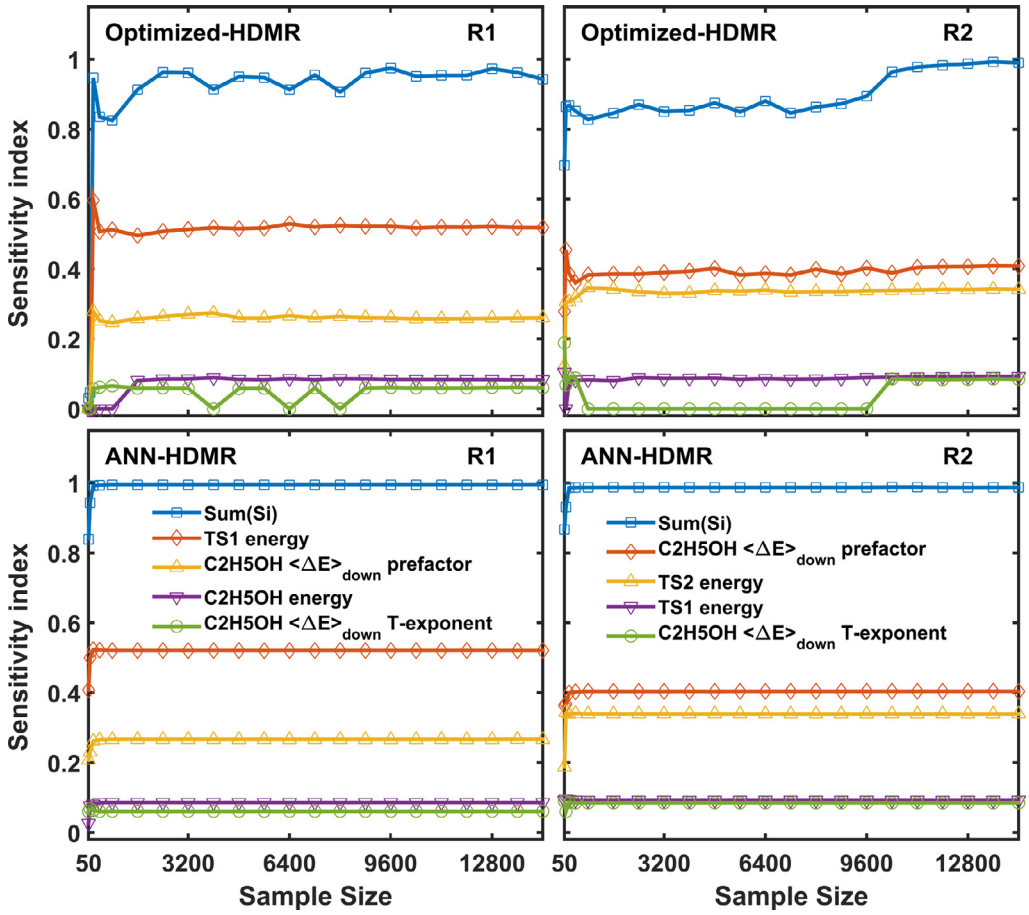

Fig. 3. The first order sensitivity indices of the four most important parameters and the sum of the first order sensitivity indices of R1 and R2 versus the original sample sizes using Optimized-HDMR and ANN-HDMR. Sum(S_i) is the sum of all first order sensitivity indices. TS1 energy, TS2 energy are the energies of transition state TS1 and TS2 respectively. C_2H_5OH $\langle\Delta E\rangle$down prefactor and C_2H_5OH $\langle\Delta E\rangle$down T-exponent are the pre-factor and temperature dependent parameter of the of the collisional energy transfer function respectively.

takes about 6000 s to obtain 200 original samples while it takes about 0.2 s to obtain 131,072 ANN samples from the well-trained ANN. Therefore, the computational cost for getting ANN samples is negligible compared to that for getting original samples. This case shows that the ANN-HDMR have great potential to perform GSA for more complex RRKM/ME simulations. To further validate the performance of ANN-HDMR, we tested this model under other nine conditions which cover the temperature and pressure ranges in the study [72]. The sensitivity results also showed that the ANN-HDMR has a fast convergence speed under these nine conditions. The sensitivity results are demonstrated in Fig. S2 provided in *Supplemental Materials.*

4.3. Premixed H_2/O_2 ignition model

4.3.1. Optimized-HDMR versus ANN-HDMR

Different from the case of Sobol' g-function, the true value of sensitivity indices for this case cannot be obtained. The sensitivity indices obtained by using DMC-HDMR with 524,288 original samples (where the sample size has been checked for convergence) were thus taken as true values. For DMC-HDMR, the maximum polynomial order for the first order component function was set to be 5 and 3 for the second order component function. The first order and second order sensitivity indices larger than 0.01 were selected as important sensitivity indices according to the results

Table 7
Sensitivity indices of important first and second order for the ignition delay time of H_2/O_2 system using Optimized-HDMR and ANN-HDMR at $P = 1.59$ bar, $T = 1000$ K and stoichiometric mixtures of H_2 and O_2.

N	Optimized-HDMR					ANN-HDMR			DMC-HDMR
	2048	4096	8192	16,384	32,768	512	1024	2048	524,288
S_{16}	0.5102	0.5097	0.5134	0.5086	0.5028	0.3494	0.5106	0.4947	0.5027
S_9	0.0903	0.0903	0.0895	0.0892	0.0892	0.0704	0.0874	0.0879	0.0892
Sum(S_i)	0.6141	0.6133	0.6129	0.6080	0.6035	0.4340	0.6129	0.5989	0.6075
$S_{9,\ 16}$	0.2259	0.2253	0.2330	0.2339	0.2597	0.3014	0.2666	0.2623	0.2656
$S_{16,\ 29}$	0.0000	0.0000	0.0000	0.0000	0.0000	0.0098	0.0085	0.0196	0.0215
$S_{11,\ 16}$	0.0097	0.0096	0.0095	0.0178	0.0179	0.0311	0.0214	0.0181	0.0178
$S_{16,\ 20}$	0.0066	0.0075	0.0063	0.0137	0.0137	0.0142	0.0132	0.0155	0.0145
Sum($S_{i,j}$)	0.2498	0.2485	0.2529	0.2704	0.2972	0.3742	0.3185	0.3303	0.3322
Sum($S_i + S_{i,j}$)	0.8639	0.8618	0.8658	0.8784	0.9008	0.8082	0.9314	0.9292	0.9397
Error	0.0800	0.0794	0.0758	0.0543	0.0228	0.2362	0.0320	0.0128	0.0000

of sensitivity analysis using DMC-HDMR. For both ANN-HDMR and Optimized-HDMR, the maximum polynomial order for the first and second order component functions were also set to be 5 and 3, respectively. For Optimized-HDMR, the correlation method was applied and the number of iterations was set to be 20 for both first and second order component functions. For ANN-HDMR, the ANN sample size was set to be 524,288, which has been verified for stable results.

The last column in Table 7 lists the important sensitivity indices calculated using DMC-HDMR with 524,288 original samples. The most important source of uncertainty is reaction 16 ($H+O_2 <=> OH+O$) whose first order term contributes about half to the overall variance of the ignition delay time. The first order term of reaction 9 ($H+O_2\ (+M) <=> HO_2\ (+M)$) contributes about 10% to the overall variance. There are four second order sensitivity indices larger than 0.01. The second order term of reaction 9 and 16 dominates the second order uncertainty of the ignition delay time.

Table 7 indicates that both Optimized-HDMR and ANN-HDMR can produce the exact important first order sensitivity indices with a small amount of original samples. For producing second order sensitivity indices, Optimized-HDMR and ANN-HDMR show a remarkable difference in respect of convergence. ANN-HDMR just needs 1024 samples to reduce the Error to <5%, while Optimized-HDMR needs 32,768 samples. Besides, Optimized-HDMR cannot accurately produce second order sensitivity index of reaction 16 and reaction 29 ($S_{16,\ 29}$) even with 32,768 original samples. The second order sensitivity index may be related to the competition between the reaction 16 ($H+O_2 <=> OH+O$) and the reaction 29 ($H_2O_2+H <=> HO_2+H_2$) for the consumption of H atom. The previous study [74] also pointed out that there was strong coupling effect between these two reactions under the same condition. It suggested that the coupling effects between these reactions are most likely to be related to the transition of the second and third explosion limits in the H_2/O_2 systems. In this case, it takes about 1000 s to obtain 1024 original samples while it only takes about 1.2 s to obtain 524,288 ANN samples for ANN-HDMR. Therefore, the computational cost for getting ANN samples is much lower than that for getting original samples.

Besides, we also tested this premixed H_2/O_2 ignition model under two additional conditions as studied in reference [74], the results are shown in Fig. S3 in *Supplemental Materials*. It also verified the good performance of ANN-HDMR.

To illustrate the practicability of ANN-HDMR for more complex model, the kinetic model for methanol oxidation is taken as an example for global sensitivity analysis. The A factors of rate coefficients are taken as input parameters and the natural logarithm of maximum mole fractions of selected species are taken as targets. The uncertainty factors of all reaction are listed in Table S2 and the simulation condition is given in Table S3 in *Supplemental Materials*. The sensitivity analysis results suggest that ANN-HDMR has a stable performance for this model, as shown in Fig. S4 in *Supplemental Materials*.

The intent of RS-HDMR is to construct low order ANOVA decomposition expression in which each term has independent effect on the output. To achieve this goal, many constraints are imposed to the minimization process. For example, if the orthonormal polynomials are used to construct RS-HDMR expression, Eqs. (16) and (17) are derived to determine coefficients α_r^i and β_{pq}^{ij} with constraints as follows:

$$\frac{1}{N}\sum_{s=1}^{N}\varphi_k\left(x_i^s\right) \approx 0,\ \ k=1,\ 2,\ \ldots \tag{26}$$

$$\frac{1}{N}\sum_{s=1}^{N}{\varphi_k}^2\left(x_i^s\right) \approx 1,\ \ k=1,\ 2,\ \ldots \tag{27}$$

$$\frac{1}{N}\sum\nolimits_{s=1}^{N}\varphi_k\left(x_i^s\right)\varphi_l\left(x_i^s\right) \approx 0 \tag{28}$$

The Monte Carlo integration error in these constraints reduces the convergent speed of RS-HDMR. On the other hand, ANN mainly cares about the accuracy of the constructed surrogate model, which explains that ANN has a faster convergent speed than HDMR. ANN-HDMR combined advantages of both methods, which leads to better performance compared to Optimized-HDMR in this case.

4.3.2. ANN-HDMR versus ANN-Sobol'

In Section 2.1, we introduced two ANN-GSA algorithms: ANN-HDMR and ANN-Sobol', but only the comparison between ANN-HDMR and Optimized-HDMR was discussed. In this section, the performances of ANN-HDMR and ANN-Sobol' will also be compared. As shown in Table 7, 2048 original samples are enough for ANN-HDMR to get accurate sensitivity indices of important first and second order terms. Therefore, 2048 original samples were used for both ANN-HDMR and ANN-Sobol' methods. For each method, we calculated the sensitivity indices with different ANN sample sizes. RS-HDMR only needs one set of ANN samples while ANN-Sobol' needs $(1+n+C_n^2)$ sets of ANN samples. For ANN-Sobol', the ANN sample size refers to the size of one set of ANN samples. Figure 4 illustrates the sum of all first and second order sensitivity indices (for which $S_i > 0.001$, $S_{i,j} > 0.002$) versus ANN sample size for ANN-HDMR and ANN-Sobol' analysis. It can be seen that the ANN sample size of $N = 65{,}536$ is sufficient for ANN-HDMR to get convergent result of the sum of all sensitivity indices while the ANN sample size of $N = 4{,}194{,}304$ is needed for ANN-Sobol' to get similar result. Table 8 shows the sensitivity indices of important terms using ANN-HDMR with an ANN sample size of $N = 65{,}536$ and using ANN-Sobol' with an ANN sample size of

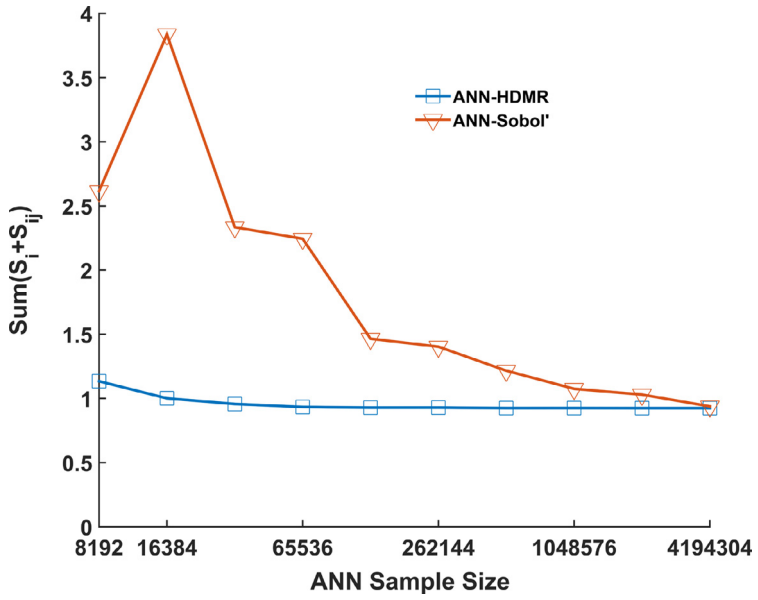

Fig. 4. The sum of all first and second order sensitivity indices (which are larger than 0.001 for first order terms, 0.002 for second order terms) versus ANN samples using ANN-HDMR and ANN-Sobol'.

Table 8
Sensitivity indices of important first and second terms using ANN-HDMR with 65,536 ANN samples and using ANN-Sobol' with 4,194,304 ANN samples. The original sample size is 2048, and the maximum polynomial order for the first order component function is 5 and for the second order component function is 3.

Method	S16	S9	Sum(S_i)	S9,16	S16,29	S11,16	S16,20	Sum($S_{i,j}$)	Sum($S_i + S_{i,j}$)	Error
DMC-HDMR	0.5025	0.0892	0.6074	0.2611	0.0204	0.0177	0.0142	0.3260	0.9334	0.0000
ANN-HDMR	0.4934	0.0877	0.5968	0.2621	0.0197	0.0179	0.0156	0.3365	0.9333	0.0139
ANN-Sobol'	0.4949	0.0874	0.5974	0.2671	0.0225	0.0173	0.0141	0.3406	0.9380	0.0180

$N = 4{,}194{,}304$. It is noticed that the results using these two methods are very close.

The results indicate that RS-HDMR and Sobol' sensitivity estimation can accurately extract the same sensitivity information from the neural network trained by the same number of original samples, but different numbers of ANN samples are needed. For Sobol' sensitivity estimation, according to Eqs. (4)–(6), the Monte Carlo integration errors of D_i and D_j are added into the calculation of second order partial variance D_{ij}. While for RS-HDMR [18], second order partial variance D_{ij} is calculated without using D_i and D_j according to Eqs. (16)–(19). This is an important reason for the slower convergent speed of Sobol' sensitivity estimation. Since the required original sample size is taken as the criteria to evaluate the convergence, ANN-HDMR and ANN-Sobol' methods have the same convergent speed but with different amount of computations for sensitivity analysis.

4.3.3. ANN-Sobol' versus Sobol' sensitivity estimation

Although Sobol' sensitivity estimation requires more samples than RS-HDMR, it has its own advantages, such as the convenience for estimating the total effect. As mentioned in Section 1, the high computational requirement hinders the application of Sobol' sensitivity estimation in practice. Taking the H_2/O_2 ignition model for example, original Sobol' sensitivity analysis needs $N*(1+n+C_n^2)$ samples to estimate the first and second order sensitivity indices. According to Fig. 4, the ANN sample size of 4,194,304 is required to ensure the sum of all the first and second order sensitivity indices less than 1, and the corresponding total sample size is up to 2.2×10^9. One original sample takes about 1 s in our computing platform, implying that about 74 years is needed to calculate all the samples, which is impractical. In contrast, 2048 original samples can provide accurate results using ANN-Sobol' with 4,194,304 ANN samples. It takes about half an hour to compute the 2048 original samples, and ANN-Sobol' needs about 1 h to calculate the sensitivity indices. The total time is less than 2 h using ANN-Sobol', which is affordable.

4.3.4. Excluding unimportant terms using residual effect

The H_2/O_2 ignition model has 33 first order sensitivity indices and 528 s order sensitivity indices. For the sensitivity analysis of ignition delay time using ANN-HDMR with 2048 original samples, if residual effect is used to exclude unimportant terms, the ANN sample size is set to be 524,288, and thresholds of 0.001, 0.005 are selected for the first and second terms, only 10 first order and 21 second order terms need to be calculated. Accounting for the 33 total effect terms, a total number of 64 terms, which is only one eighth of the original terms, are required to be computed using the residual effect to exclude unimportant terms. The effect of cost reduction of residual effect will be more pronounced if the system has more input parameters or higher order effects need to be considered. For example, to estimate the sensitivity indices up to the third order for the above case, 6017 terms (33 first order + 528 second order + 5456 third order terms) need to be computed. Using residual effect with thresholds of 0.001 for the first order and 0.005 for the second and third order terms to exclude unimportant terms, only a total of 81 terms (33 total effect + 10 first order + 21 second order + 17 third order terms) need to be calculated, which is about one seventieth of the original terms.

5. Conclusions

This work presents an ANN based surrogate model formulation for Sobol' sensitivity estimation and high-dimensional model rep-

resentation (HDMR). Particularly, ANN-HDMR replaces the single-step surrogate process with a two-step process. First, an artificial neural network is created as a surrogate for the detailed model, and then the RS-HDMR is constucted using the artificial neural network. By coupling the advantage of ANN for fast convergence and RS-HDMR for direct sensitivity indices calculation, the proposed double-layer surrogate model method (ANN-HDMR) has been proved to have high computational efficiency for global sensitivity analysis. In addition, the "residual effect" was introduced to determine the important terms which need to be taken into account, and this method can greatly reduce the calculation especially when the model has a large number of input parameters and high order effects need to be estimated. A fully functional and user friendly program integrating the methods proposed in this work was developed and could be provided to potential users.

Acknowledgments

This work is supported by National Natural Science Foundation of China (91541113, U1332208). We greatly appreciate Professor Alison Tomlin for her helpful discussions and her critical inspections in using the GUI-HDMR code, and also express gratitude to Dr. Feng Zhang, Zhen Lu, Wenyu Sun, Tao Tao, Ruzheng Zhang and Jiaxing Wang for their helpful discussions.

Supplementary materials

Supplementary material associated with this article can be found, in the online version, at doi:10.1016/j.combustflame.2016.03.028.

References

[1] H. Wang, D.A. Sheen, Combustion kinetic model uncertainty quantification, propagation and minimization, Prog. Energy Combust. Sci. 47 (2015) 1–31.
[2] W.L. Oberkampf, C.J. Roy, Verification and validation in scientific computing, Cambridge University Press, Cambridge, 2010.
[3] A. Saltelli, S. Tarantola, F. Campolongo, M. Ratto, Sensitivity analysis in practice: a guide to assessing scientific models, John Wiley & Sons Ltd, Chichester, 2004.
[4] R.J. Kee, F.M. Rupley, J.A. Miller Chemkin-II, A Fortran chemical kinetics package for the analysis of gas-phase chemical kinetics SAND-89-8009, Sandia National Labs., Livermore, CA (USA), 1989.
[5] T. Turányi, KINAL—a program package for kinetic analysis of reaction mechanisms, Comput. Chem. 14 (1990) 253–254.
[6] D.M.N. Goodwin, H.S. Moffat, R. Cantera: A suite of object-oriented software tools for problems involving chemical kinetics, thermodynamics, and/or transport processes. 2014, http://sourceforge.net/projects/cantera/.
[7] H. Pitsch, FlameMaster v3. 1: A C++ computer programe for 0D combustion and 1D laminar flame calculations. 1998, http://web.stanford.edu/~hpitsch/FlameMaster.html.
[8] A. Cuoci, A. Frassoldati, T. Faravelli, E. Ranzi, A computational tool for the detailed kinetic modeling of laminar flames: application to C_2H_4/CH_4 coflow flames, Combust. Flame 160 (2013) 870–886.
[9] A. Cuoci, A. Frassoldati, T. Faravelli, E. Ranzi, OpenSMOKE++: an object-oriented framework for the numerical modeling of reactive systems with detailed kinetic mechanisms, Comput. Phys. Commun. 192 (2015) 237–264.
[10] A. Saltelli, M. Ratto, S. Tarantola, F. Campolongo, Sensitivity analysis for chemical models, Chem. Rev. 105 (2005) 2811–2828.
[11] A.S. Tomlin, The role of sensitivity and uncertainty analysis in combustion modelling, Proc. Combust. Inst. 34 (2013) 159–176.
[12] I.M. Sobol', Sensitivity estimates for nonlinear mathematical models, Matem. Modelirovanie 2 (1990) 112–118.
[13] T. Homma, A. Saltelli, Importance measures in global sensitivity analysis of nonlinear models, Reliab. Eng. Syst. Saf. 52 (1996) 1–17.
[14] I.M. Sobol', Global sensitivity indices for nonlinear mathematical models and their Monte Carlo estimates, Math. Comput. Simul. 55 (2001) 271–280.
[15] H. Rabitz, Ö.F. Aliş, General foundations of high-dimensional model representations, J. Math. Chem. 25 (1999) 197–233.
[16] H. Rabitz, Ö.F. Aliş, J. Shorter, K. Shim, Efficient input–output model representations, Comput. Phys. Commun. 117 (1999) 11–20.
[17] Ö. Alış, H Rabitz, Efficient implementation of high dimensional model representations, J. Math. Chem. 29 (2001) 127–142.
[18] G. Li, S.-W. Wang, H. Rabitz, Practical approaches to construct RS-HDMR component functions, J. Phys. Chem. A 106 (2002) 8721–8733.
[19] M.J.W. Jansen, Analysis of variance designs for model output, Comput. Phys. Commun. 117 (1999) 35–43.
[20] A. Saltelli, P. Annoni, I. Azzini, F. Campolongo, M. Ratto, S. Tarantola, Variance based sensitivity analysis of model output. Design and estimator for the total sensitivity index, Comput. Phys. Commun. 181 (2010) 259–270.
[21] G. Li, H. Rabitz, S.W. Wang, P.G. Georgopoulos, Correlation method for variance reduction of Monte Carlo integration in RS-HDMR, J. Comput. Chem. 24 (2003) 277–283.
[22] G. Li, H. Rabitz, Ratio control variate method for efficiently determining high-dimensional model representations, J. Comput. Chem. 27 (2006) 1112–1118.
[23] T. Ziehn, A.S. Tomlin, Global sensitivity analysis of a 3D street canyon model—Part I: the development of high dimensional model representations, Atmos. Environ. 42 (2008) 1857–1873.
[24] T. Ziehn, A.S. Tomlin, A global sensitivity study of sulfur chemistry in a premixed methane flame model using HDMR, Int. J. Chem. Kinet. 40 (2008) 742–753.
[25] T. Ziehn, A.S. Tomlin, GUI–HDMR—a software tool for global sensitivity analysis of complex models, Environ. Modell. Softw. 24 (2009) 775–785.
[26] A.K. Jain, J. Mao, K.M. Mohiuddin, Artificial neural networks: a tutorial, Computer 29 (1996) 31–44.
[27] A.K. Jain, R.P.W. Duin, M. Jianchang, Statistical pattern recognition: a review, IEEE Trans. Pattern Anal. Mach. Intell. 22 (2000) 4–37.
[28] G. Hinton, D. Li, Y. Dong, G.E. Dahl, A. Mohamed, N. Jaitly, A. Senior, V. Vanhoucke, P. Nguyen, T.N. Sainath, B. Kingsbury, Deep neural networks for acoustic modeling in speech recognition: the shared views of four research groups, IEEE Signal Process. Mag. 29 (2012) 82–97.
[29] C. Srivaree-ratana, A. Konak, A.E. Smith, Estimation of all-terminal network reliability using an artificial neural network, Comput. Oper. Res. 29 (2002) 849–868.
[30] A.A. Chojaczyk, A.P. Teixeira, L.C. Neves, J.B. Cardoso, C. Guedes Soares, Review and application of artificial neural networks models in reliability analysis of steel structures, Struct. Saf. 52 (2015) 78–89.
[31] S. Dreiseitl, L. Ohno-Machado, Logistic regression and artificial neural network classification models: a methodology review, J. Biomed. Inf. 35 (2002) 352–359.
[32] A.S. Britto Jr, R. Sabourin, L.E.S. Oliveira, Dynamic selection of classifiers—a comprehensive review, Pattern Recognit 47 (2014) 3665–3680.
[33] F. Amato, A. López, E.M. Peña-Méndez, P. Vaňhara, A. Hampl, J. Havel, Artificial neural networks in medical diagnosis, J. Appl. Biomed. 11 (2013) 47–58.
[34] P.J.G. Lisboa, A review of evidence of health benefit from artificial neural networks in medical intervention, Neural Netw 15 (2002) 11–39.
[35] K.J. Hunt, D. Sbarbaro, R. Żbikowski, P.J. Gawthrop, Neural networks for control systems—a survey, Automatica 28 (1992) 1083–1112.
[36] J. Na, X. Ren, C. Shang, Y. Guo, Adaptive neural network predictive control for nonlinear pure feedback systems with input delay, J. Process Control 22 (2012) 194–206.
[37] F. Christo, A. Masri, E. Nebot, T. Turanyi, Utilising artificial neural network and repro-modelling in turbulent combustion, 1995. IEEE International Conference on Neural Networks, Proceedings, IEEE (1995), pp. 911–916.
[38] F.C. Christo, A.R. Masri, E.M. Nebot, Artificial neural network implementation of chemistry with PDF simulation of H_2/CO_2 flames, Combust. Flame 106 (1996) 406–427.
[39] F.C. Christo, A.R. Masri, E.M. Nebot, S.B. Pope, An integrated PDF/neural network approach for simulating turbulent reacting systems, Symp. (Int.) Combust. 26 (1996) 43–48.
[40] J.A. Blasco, N. Fueyo, C. Dopazo, J. Ballester, Modelling the temporal evolution of a reduced combustion chemical system with an artificial neural network, Combust. Flame 113 (1998) 38–52.
[41] J.A. Blasco, N. Fueyo, J.C. Larroya, C. Dopazo, Y.J. Chen, A single-step time-integrator of a methane–air chemical system using artificial neural networks, Comput. Chem. Eng. 23 (1999) 1127–1133.
[42] J.Y. Chen, J.A. Blasco, N. Fueyo, C. Dopazo, An economical strategy for storage of chemical kinetics: fitting in situ adaptive tabulation with artificial neural networks, Proc. Combust. Inst. 28 (2000) 115–121.
[43] Y. Choi, J.Y. Chen, Fast prediction of start-of-combustion in HCCI with combined artificial neural networks and ignition delay model, Proc. Combust. Inst. 30 (2005) 2711–2718.
[44] F. Flemming, A. Sadiki, J. Janicka, LES using artificial neural networks for chemistry representation, Int. J. Prog. Comput. Fluid Dyn. 5 (2005) 375–385.
[45] M. Ihme, A.L. Marsden, H. Pitsch, Generation of optimal artificial neural networks using a pattern search algorithm: application to approximation of chemical systems, Neural Comput 20 (2008) 573–601.
[46] M. Ihme, C. Schmitt, H. Pitsch, Optimal artificial neural networks and tabulation methods for chemistry representation in LES of a bluff-body swirl-stabilized flame, Proc. Combust. Inst. 32 (2009) 1527–1535.
[47] A.K. Chatzopoulos, S. Rigopoulos, A chemistry tabulation approach via rate–controlled constrained equilibrium (RCCE) and artificial neural networks (ANNs), with application to turbulent non-premixed $CH_4/H_2/N_2$ flames, Proc. Combust. Inst. 34 (2013) 1465–1473.
[48] H. Mirgolbabaei, T. Echekki, A novel principal component analysis-based acceleration scheme for LES–ODT: an a priori study, Combust. Flame 160 (2013) 898–908.
[49] T. Turányi, A.S. Tomlin, Analysis of kinetic reaction mechanisms, Springer, 2014.
[50] D.E. Rumelhart, G.E. Hinton, R.J. Williams, Learning representations by back-propagating errors, Nature 323 (1986) 533–536.
[51] M.T. Hagan, M.B. Menhaj, Training feedforward networks with the Marquardt algorithm, IEEE Trans. Neural Netw. 5 (1994) 989–993.

[52] B. Yegnanarayana, Artificial neural networks, PHI Learning Pvt. Ltd., 2009.
[53] P. Koprinkova-Hristova, V. Mladenov, N.K. Kasabov, Artificial neural networks: methods and applications in bio-/neuroinformatics, Springer, 2014.
[54] W. Hoeffding, A class of statistics with asymptotically normal distribution, Ann. Math. Statist. 19 (1948) 293–325.
[55] M.D. McKay, Nonparametric variance-based methods of assessing uncertainty importance, Reliab. Eng. Syst. Saf. 57 (1997) 267–279.
[56] G. Li, C. Rosenthal, H. Rabitz, High dimensional model representations, J. Phys. Chem. A 105 (2001) 7765–7777.
[57] A. Saltelli, I.M. Sobol, Sensitivity analysis for nonlinear mathematical models: numerical experience, Matem. Modelirovanie 7 (1995) 16–28.
[58] A. Saltelli, I.M. Sobol, About the use of rank transformation in sensitivity analysis of model output, Reliab. Eng. Syst. Saf. 50 (1995) 225–239.
[59] A. Marrel, B. Iooss, F. Van Dorpe, E. Volkova, An efficient methodology for modeling complex computer codes with Gaussian processes, Comp. Stat. Data Anal. 52 (2008) 4731–4744.
[60] A. Marrel, B. Iooss, B. Laurent, O. Roustant, Calculations of Sobol indices for the Gaussian process metamodel, Reliab. Eng. Syst. Saf. 94 (2009) 742–751.
[61] S. Kucherenko, B. Feil, N. Shah, W. Mauntz, The identification of model effective dimensions using global sensitivity analysis, Reliab. Eng. Syst. Saf. 96 (2011) 440–449.
[62] M. Ratto, A. Pagano, P. Young, State dependent parameter metamodelling and sensitivity analysis, Comput. Phys. Commun. 177 (2007) 863–876.
[63] M. Brouard, M.T. Macpherson, M.J. Pilling, Experimental and RRKM modeling study of the methyl+hydrogen atom and deuterium atom reactions, J. Phys. Chem. 93 (1989) 4047–4059.
[64] S.J. Klippenstein, Variational optimizations in the Rice–Ramsperger–Kassel–Marcus theory calculations for unimolecular dissociations with no reverse barrier, J. Chem. Phys. 96 (1992) 367–371.
[65] H. Somnitz, R. Zellner, Theoretical studies of unimolecular reactions of C 2–C 5 alkoxy radicals. Part II. RRKM dynamical calculations, Phys. Chem. Chem. Phys. 2 (2000) 1907–1918.
[66] J.A. Miller, S.J. Klippenstein, Master equation methods in gas phase chemical kinetics, J. Phys. Chem. A 110 (2006) 10528–10544.
[67] I. Suh, J. Zhao, R. Zhang, Unimolecular decomposition of aromatic bicyclic alkoxy radicals and their acyclic radicals, Chem. Phys. Lett. 432 (2006) 313–320.
[68] W.S. McGivern, I.A. Awan, W. Tsang, J.A. Manion, Isomerization and decomposition reactions in the pyrolysis of branched hydrocarbons: 4-methyl-1-pentyl radical, J. Phys. Chem. A 112 (2008) 6908–6917.
[69] C.F. Goldsmith, S.J. Klippenstein, W.H. Green, Theoretical rate coefficients for allyl+HO_2 and allyloxy decomposition, Proc. Combust. Inst. 33 (2011) 273–282.
[70] E.E. Dames, D.M. Golden, Master equation modeling of the unimolecular decompositions of hydroxymethyl (CH_2OH) and methoxy (CH_3O) radicals to formaldehyde (CH_2O)+H, J. Phys. Chem. A 117 (2013) 7686–7696.
[71] C.F. Goldsmith, A.S. Tomlin, S.J. Klippenstein, Uncertainty propagation in the derivation of phenomenological rate coefficients from theory: a case study of *n*-propyl radical oxidation, Proc. Combust. Inst. 34 (2013) 177–185.
[72] L. Xing, S. Li, Z. Wang, B. Yang, S.J. Klippenstein, F. Zhang, Global uncertainty analysis for RRKM/master equation based kinetic predictions: a case study of ethanol decomposition, Combust. Flame 162 (2015) 3427–3436.
[73] S.H. Robertson, R. Shannon, P.W. Seakins, M.J. Pilling, MESMER (Master Equation Solver for Multi-Energy Well Reactions), 2008-2013; an object oriented C++ program implementing master equation methods for gas phase reactions with arbitrary multiple well. 2013, http://sourceforge.net/projects/mesmer.
[74] M.J. Davis, R.T. Skodje, A.S. Tomlin, Global sensitivity analysis of chemical-kinetic reaction mechanisms: construction and deconstruction of the probability density function, J. Phys. Chem. A 115 (2011) 1556–1578.
[75] A.A. Konnov, Remaining uncertainties in the kinetic mechanism of hydrogen combustion, Combust. Flame 152 (2008) 507–528.
[76] I.M. Sobol', On the distribution of points in a cube and the approximate evaluation of integrals, USSR Comput. Math. Math. Phys. 7 (1967) 86–112.